Journal of Computer Assisted Tomography
18(1):119–125, January/February

Effect of Water Fraction in Selection of Optimal TI Value for STIR Sequences

Hideharu Sugimoto, Osamu Sakai, Takeshi Shinozaki, Tadashi Ohsawa, and Tokunori Kimura

Objective: This article describes the effect of the water fraction in the selection of the optimal TI value in a STIR sequence. This effect has been given little consideration in previous studies.

Materials and Methods: Therefore, using both STIR combined with the Dixon method (opposed-phase STIR) and conventional STIR (in-phase STIR), we have investigated the effect of the water fraction in the selection of an optimal TI value for the STIR sequence.

Results: Our findings have indicated that the water protons rather than the olefinic protons ($-CH=CH-$) play a major role in the opposed-phase effect in vivo.

Conclusion: Thus, it has been concluded that the most effective fat suppression can be achieved when the intravoxel phase cancellation effect between the water and lipid protons is maximal, rather than when the longitudinal magnetization of the lipid protons is minimal.

Index Terms: Magnetic resonance imaging, techniques—Inversion recovery—Magnetic resonance imaging.

In the short inversion time inversion recovery (STIR) sequence, the inversion time (TI) is adjusted to suppress the longitudinal magnetization of protons present in adipose tissue (1). In such instances, the TI value is chosen either by a simple calculation using the published TI value of adipose tissue (2,3) or by imaging volunteers with different TIs (4). In this regard, TI tuning using spectral display has recently been reported as being useful in selecting the optimal TI for the suppression of fat protons (5). However, it must be kept in mind that lipid protons are not the sole constituent of protons in adipose tissue.

Water also constitutes a part of adipose tissue, and it has been extensively investigated in relation to measurements of adipose tissue mass. The mean ± SD water fraction of the human body is said to be 15.3 ± 5.0%, and it does not vary significantly in any part of the body (Fig. 1) (6). Therefore, these water protons in the adipose tissue should not be ignored when designing a pulse sequence for proton chemical shift imaging. If the aim is to achieve a complete suppression of normal adipose tissue, then both water and lipid protons should be suppressed.

In the magnitude mode, the phase information of the IR sequence is ignored in the reconstruction process. However, when two or more kinds of protons precessing with different frequencies are present in the voxel, the phase effect is bound to affect the signal intensity. Herein, we describe the effect of the water fraction in the selection of the optimal TI value in a STIR sequence, an effect that has been given little consideration in previous studies (1–5).

MATERIALS AND METHODS

Theoretical Signal Intensity Analysis

In the IR sequence, the initial longitudinal magnetization ($+Mz$) is tipped toward a negative direction ($-Mz$). Further, it is assumed that in the opti-

From the Department of Radiology, Jichi Medical School (H. Sugimoto, O. Sakai, T. Shinozaki and T. Ohsawa), and Toshiba Nasu Works (T. Kimura), Tochigi-Ken, Japan. Address correspondence and reprint requests to Dr. H. Sugimoto at Department of Radiology, Jichi Medical School, Minamikawachi-Machi, Kawachi-Gun, Tochigi-Ken 329-04, Japan.

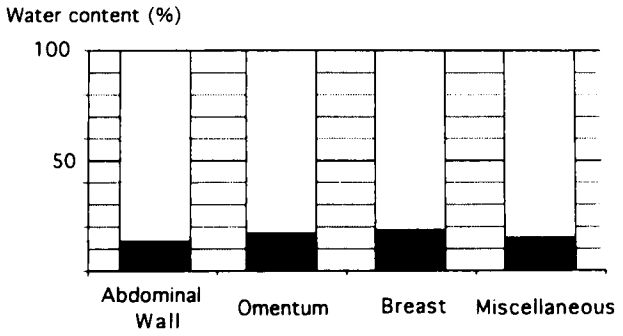

FIG. 1. Mean water fraction of adipose tissue from abdominal wall, omentum, breast, and miscellaneous sites (adapted from ref. 6).

mal TI (TI_{op}), protons of adipose tissue have no net longitudinal magnetization ($|Mz_{adipose}| = 0$) at their exposure to a 90° pulse for SE acquisition. However, because ~15% of adipose tissue is water (6), the net longitudinal magnetization in the voxel is not zero ($|Mz_{water}| \neq 0$) when the TI is selected to suppress the lipid protons ($-CH_2-$) (point a in Fig. 2a). Therefore, when the TI is shorter than the zero cross-point of the lipid protons, the longitudinal magnetization of the lipid protons in the voxel (Mz_{lipid}) is in the same direction as that of the water protons (Mz_{water}) (point b in Fig. 2b). Conversely, when the TI is longer than the zero cross-point of the lipid protons, then Mz_{lipid} is positive and in

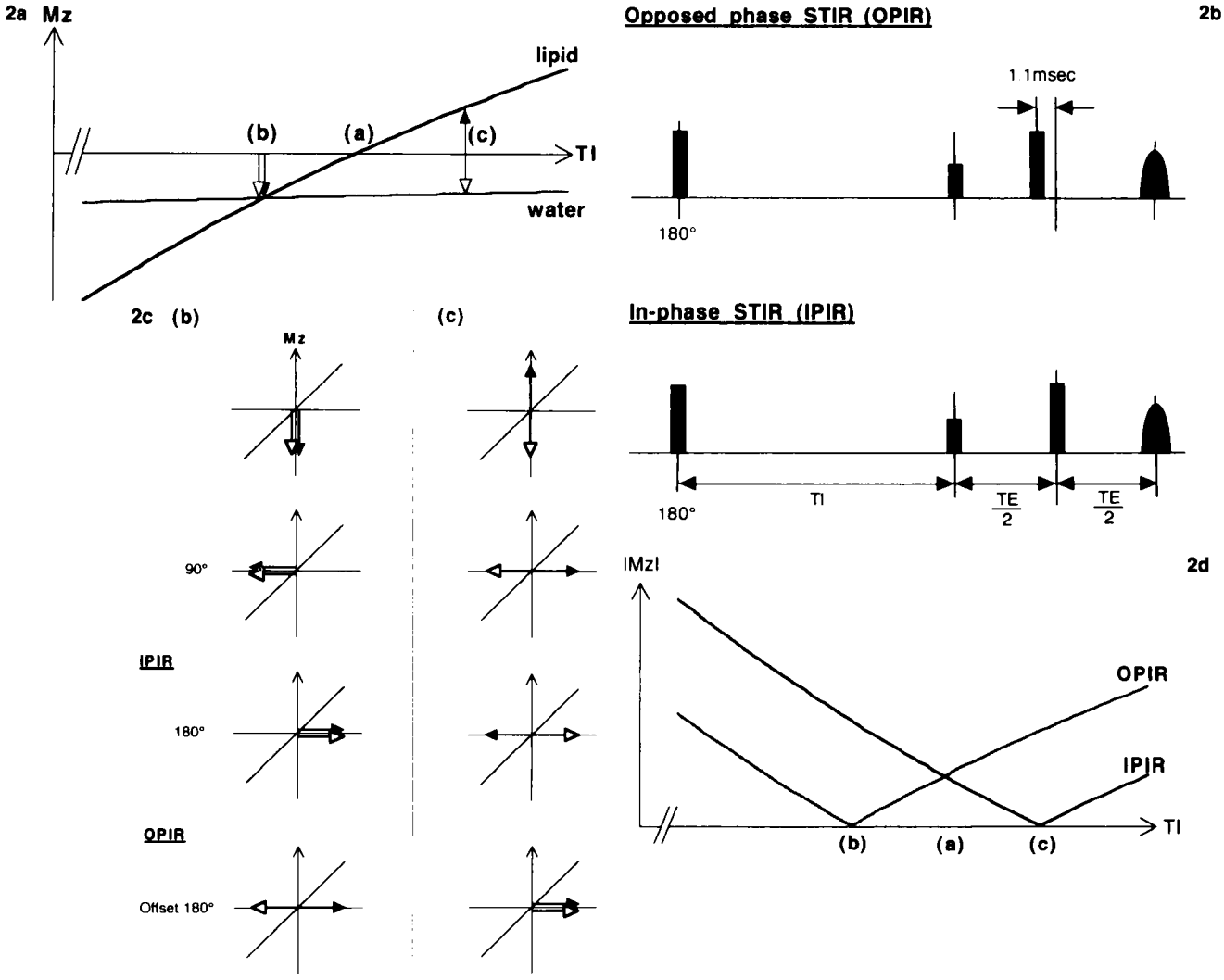

FIG. 2. a: Longitudinal magnetization of water and lipid protons in the STIR sequence. Point a represents the zero cross-point of the lipid protons. Points b and c represent the TIs at which $|Mz_{water}|$ equals $|Mz_{lipid}|$. **b:** Pulse diagram of the OPIR and IPIR sequences. Instead of the read gradient being shifted from TE as in Dixon's original description, a 180° refocusing pulse was shifted to obtain an opposed image in the OPIR sequence. **c:** The magnetization vectors of the water and lipid (aliphatic) protons in the OPIR and IPIR sequences. The left and right columns represent magnetization at points b and c of (a). In both sequences, the water and lipid protons are brought to either the opposed phase or in phase at the time of data acquisition. **d:** The OPIR and IPIR signal intensity profile in the magnitude reconstruction mode. Points a, b, and c correspond to these points in (a). The intensity profiles of OPIR and IPIR are identical, but the OPIR signal has shifted toward the negative direction of the TI axis. The OPIR signal intensity is much lower than the IPIR signal when the TI is shorter than the OPIR-IPIR intersection.

opposition to the direction of Mz_{water} (point c in Fig. 2a).

Opposed-Phase STIR

The asymmetric SE (ASE) technique was originally described by Dixon (7) as being a simple spectroscopic imaging technique; by this method, when an appropriate offset value ($\tau/2$) of the 180° refocusing pulse is chosen, opposed images of the fat and water protons can be obtained. The opposed-phase STIR (OPIR) is a modified STIR sequence in which the ASE is used to acquire the Hahn echo signal (Fig. 2b). Therefore, should the TI be shorter than the zero cross-point of the lipid protons, the OPIR will yield opposed images of the water and lipid protons (Fig. 2c, left). However, the signal intensity of the adipose tissue is much lower than that of in-phase STIR (IPIR) images, since the net OPIR magnetization ($|Mz_{water}| - |Mz_{lipid}|$) is lower than that of the IPIR ($|Mz_{water}| + |Mz_{lipid}|$). Conversely, when the TI is longer than the zero cross-point of the lipid protons, the net OPIR magnetization is ($|Mz_{water}| + |Mz_{lipid}|$) (Fig. 2c, right). This is because the ASE converts the out-of-phase lipid and water protons to in-phase at the time of signal acquisition. The net IPIR magnetization in this condition could be ($|Mz_{water}| - |Mz_{lipid}|$). Therefore, OPIR provides less effective fat suppression than does IPIR when the TI is longer than the zero cross-point of the lipid protons. Figure 2d shows the expected OPIR and IPIR signal intensity profiles. Points a, b, and c correspond to the same points shown in Fig. 2a (Appendix). (In this section, water protons were used, for the sake of simplicity, to represent protons in the opposed phase to the aliphatic protons. For a more complete description, the contribution of olefinic protons must be described; however, at the zero signal axis, their contribution would be small.)

MRI

All studies were performed with an MRT 200 FX/II (Toshiba, Tokyo) equipped with a superconducting magnet operating at 1.5 T field strength. The STIR images consisted of a TR of 2,000 ms and a TE of 30 ms. Further, a TI from 130 to 170 ms was used. To eliminate cross-talk, a single slice with a section thickness of 5 mm was obtained. The field of view was 25–35 cm, and the image matrix was 128 × 256 with one excitation. First-order gradient moment nulling was applied in both slicing and reading gradients. The total imaging time of each sequence was 4.3 min. All images were reconstructed in the magnitude mode. In this study, the offset of the OPIR 180° pulse ($\tau/2$) was set at 1.1 ms, giving a half-cycle change for the 220 Hz chemical shift.

Volunteers

Six healthy, nonobese volunteers (3 men and 3 women, 22–50 years old) were studied to evaluate IPIR and OPIR signal characteristics. In four of these volunteers, the axial section through the orbit was obtained. A coronal section through the neck (at the level of the deep cervical lymph node chain) was obtained from one volunteer and through the pelvis (at the level of the vagina) from another. For imaging of the orbit, a quadrature coil was used for the transmitter and receiver. For imaging of the neck, a specialized neck coil was used as a receiver. For imaging of the pelvis, a body coil was used for the transmitter and receiver. With TR (2,000 ms) and TE (30 ms) kept constant, TI was set at 130, 140, 150, 160, and 170 ms. Both IPIR and OPIR were obtained in the same settings of the TR, TE, and TI.

Retrobulbar fat, subcutaneous fat, and perirectal fat were used to represent adipose tissue in each region. The signal intensity of adipose tissue was measured by using a cursor-defined region of interest and plotted as a function of the TI. These points were then interpolated and the crossover point of the OPIR and IPIR was obtained from graph software (CricketGraph, version 1.3.1).

Patients

To confirm an intravoxel phase cancellation effect, 27 patients were studied using both the IPIR and the OPIR sequences. The imaging areas were the orbit (13), neck (12), pelvis (1), and hips (1). The number of cases for each TI is shown in Table 1. The same coils used in the study of volunteers were used for the imaging of the orbit, neck, and pelvis. For imaging of the hip joint, 15 cm surface coils with Helmholz configurations were used. The study was performed following conventional T1-weighted and/or T2-weighted imaging. In this system, 8–10 slices could be obtained in the TI range. The IPIR

TABLE 1. *No. of cases for variety of TIs*

	TI (ms)						
	120	130	140	150	160	170	Total
No. cases	4	4	8	5	2	4	27
Region							
Orbit		1	6	3	2	1	13
Neck	3	3	2	1		3	12
Pelvis				1			1
Hip	1						1

and OPIR imaging parameters were otherwise identical to those in the study of the volunteers.

Signal difference/noise ratio (SD/N) was calculated between lesions with the most conspicuous appearance and the surrounding adipose tissue. The SD/N was defined by the following formula: SD/N = $(S_l - S_a)$/noise, wherein S_l is the signal intensity of lesions and S_a is the signal intensity of adipose tissue. By dividing the SD/N of the OPIR by the SD/N of the IPIR $[(SD/N)_{OPIR}/(SD/N)_{IPIR}]$, the relative SD gain in the OPIR (G_{OPIR}) was obtained.

RESULTS

Volunteers

The interpolated signal intensities of adipose tissue in IPIR and OPIR crossed each other from 150.2 to 157.1 ms of the TI (average 154.0 ± 2.9 ms) (Fig. 3a). When the TI was shorter than the intersection, OPIR was more effective in suppressing the adipose signal than IPIR. Conversely, when the TI was longer than the intersection, IPIR proved to be more effective (Fig. 3 and c). In both sequences, the nadir of the intensity profile was near the noise level. No significant difference was noted in the configuration of the intensity profile among the locations. Visual inspection revealed that OPIR and IPIR were similar in terms of fat suppression when the TI was 150 ms.

Patients

The G_{OPIR} at each TI is shown in Fig. 3. It was highest at TI = 140 (ms) (Fig. 4). The standard

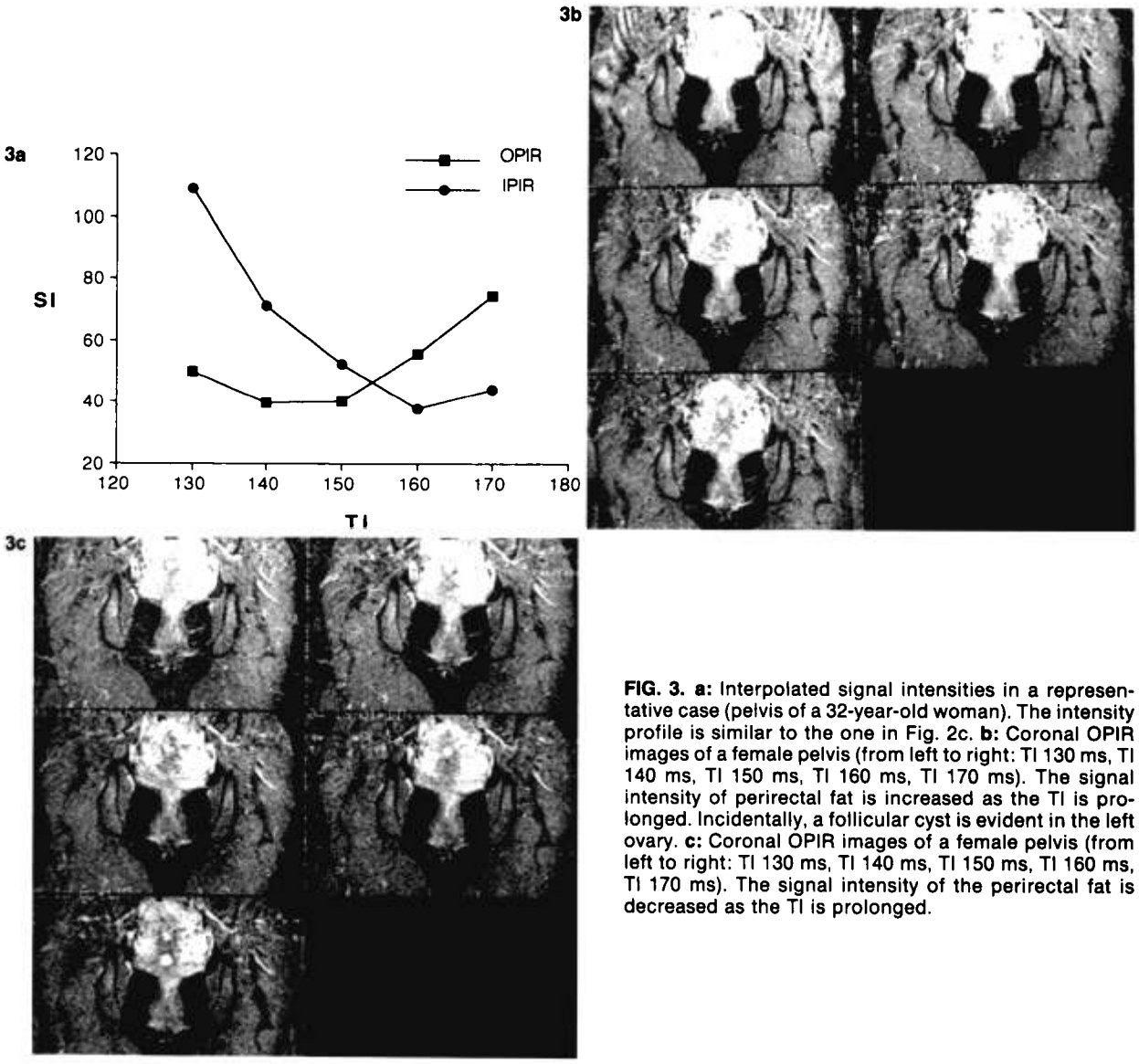

FIG. 3. a: Interpolated signal intensities in a representative case (pelvis of a 32-year-old woman). The intensity profile is similar to the one in Fig. 2c. **b:** Coronal OPIR images of a female pelvis (from left to right: TI 130 ms, TI 140 ms, TI 150 ms, TI 160 ms, TI 170 ms). The signal intensity of perirectal fat is increased as the TI is prolonged. Incidentally, a follicular cyst is evident in the left ovary. **c:** Coronal OPIR images of a female pelvis (from left to right: TI 130 ms, TI 140 ms, TI 150 ms, TI 160 ms, TI 170 ms). The signal intensity of the perirectal fat is decreased as the TI is prolonged.

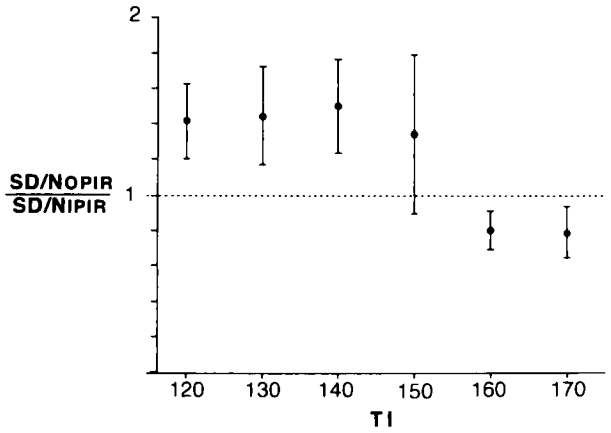

FIG. 4. Diagram of TI versus G_{OPIR}. Vertical line represents a 1 SD error bar.

deviation of G_{OPIR} was the least at TI = 120. At a TI of 160 or 170 ms, the G_{OPIR} was <1 because of better fat suppression with IPIR than with OPIR. The $(SD/N)_{OPIR}$ was found to be ~50% higher than the $(SD/N)_{IPIR}$ at TI = 140. On the other hand, the $(SD/N)_{OPIR}$ was 20% lower than the $(SD/N)_{IPIR}$ when the TI was 160 or 170 ms.

Figures 5 and 6 were representative cases. The images were displayed with the same window level and width to show the degree of IPIR and OPIR fat suppression. Each image appeared identical, except for a better suppression of adipose tissue on OPIR than on IPIR in Fig. 5 and a better suppression on IPIR than on OPIR in Fig. 6.

FIG. 6. Coronal orbital images. A 54-year-old woman with right pseudotumor. TI = 160 ms. In contrast to the previous case, more effective fat suppression was demonstrated on IPIR **(top)** than on OPIR **(bottom).** Note almost total absence of signal from the orbital fat on IPIR.

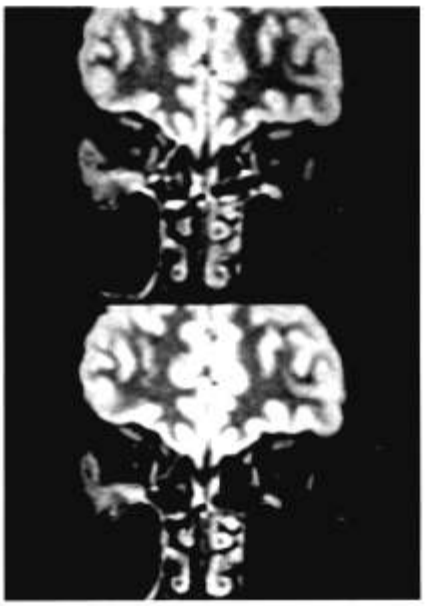

FIG. 5. Coronal orbital images. A 41-year-old man with right orbital pseudotumor. TI = 130 ms. More effective fat suppression was achieved on OPIR **(bottom)** than on IPIR **(top).**

DISCUSSION

Several methods are used to determine the TI_{op} in the STIR sequence. In one method, the TI_{op} is calculated by using the published T1 values for adipose tissue. The main drawback of this method, however, is the wide disparity in the reported T1 values (8,9). But more precise measurements of tissue relaxation times have recently been reported in an animal study (10), so that this disparity may become less of a problem in future human studies. The second method is to perform a preliminary study in volunteers or in patients to determine the TI_{op} of a given system by taking multiple images while changing the TI values (4). However, the TI_{op} may differ among individuals or even change within the same person, depending on the body site (5,11). The third method is to use a TI tuning technique (11), through which the TI that produces the lowest fat peak is determined by observing the fat signal peak during manual increment of the TI. It has been noted, however, that the TI selected by means of TI tuning is not identical to the TI that produced the lowest experimentally measured fat intensity (5). Often the TI selected by TI tuning is shorter than the TI of the minimal fat intensity.

Based on the results of our study, it is apparent that the discordance in the TI tuning method is due to the presence of protons precessing at the same frequency as water in the adipose tissue. Because TI tuning provides the TI values to suppress the aliphatic protons selectively, these TIs do not suppress the entire longitudinal magnetization in the voxel. The TI that produces the lowest measured

fat intensity corresponds to point a in Fig. 2a. The minimal fat intensity is given at point c. Therefore, TI tuning gives a shorter TI than a TI of minimal fat intensity.

Adipose tissue has two kinds of protons that precess at the same or almost the same frequency of water protons: water protons and the olefinic fat protons of the lipid molecules. With respect to the latter, the phase effect of olefinic fat ($-CH=CH-$) has been recently investigated with a combined chemical shift and phase-selective sequence in vitro (12). Although the study included some clinical data, it did not support the concept that all protons with an opposed phase to aliphatic protons are really olefinic fat protons in human adipose tissue. Approximately 5% of the fatty tissue protons are composed of olefinic fat protons, whereas ~15% of the content of adipose tissue is water (6) (Fig. 1). Further, the TI of the $-CH=$ proton (339 ± 21 ms) is much closer to that of the $-CH_2-$ proton (257 ± 7 ms) than to that of the water proton (963 ± 77 ms) (13). Therefore, water protons must play a quantitatively major role in the opposed-phase effect at the TIs used in this study.

As the pulse sequence for fat suppression is originated on the basis of phase contrast, chemical saturation (frequency-selective pulse), or the relaxation rate mechanism, and since each of these methods has its disadvantages, a hybrid approach is recommended (14). Therefore, from this and other (12) studies, a method for devising a hybrid approach for fat suppression is schematically summarized in Fig. 7. When using the chemical presaturation technique, magnetization with frequencies different from aliphatic protons does not remain suppressed. However, by combining the chemical saturation method and the phase contrast method, it is possible to suppress the entire longitudinal magnetization in adipose tissue. In the STIR sequence, residual longitudinal magnetization of adipose tissue due to an imperfect TI setting can be cancelled by the phase contrast technique.

Although both IPIR and OPIR can cause the same degree of adipose suppression at the appropriate TI setting, OPIR has several advantages over IPIR because of its shorter TI. First, OPIR signal/noise ratio is better than that of IPIR. Further, the improvement of the $(SD/N)_{OPIR}$ in the shorter TIs is greater than that of the $(SD/N)_{IPIR}$ in the longer TIs, because a larger longitudinal magnetization of the water protons in the lesions is available at shorter than at longer TIs. Second, more slices can be obtained in OPIR than in IPIR.

Paramagnetic contrast agents are not recommended with a relatively long TR STIR sequence, since they shorten both the T1 and T2 relaxation times (1,15). However, a recent study has indicated that Gd-DTPA enhancement is achievable with a short TR STIR (16). Therefore, a short TR STIR

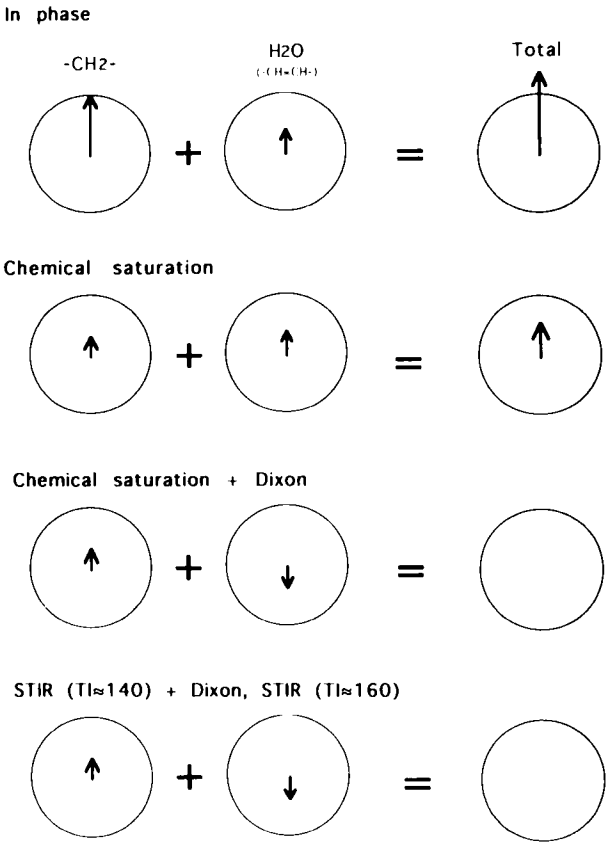

FIG. 7. Diagram of the mechanisms involved in the fat suppression sequences.

combined with the Dixon method may be the most appropriate sequence for fat suppression, unless effective chemical saturation is achievable with certain specialized equipment.

In bone marrow imaging, a susceptibility-induced signal loss due to bone trabeculae can present a problem in OPIR. However, this effect is small if the offset TE value is in the range of 1.1 ms (17).

To conclude, TI tuning does not give the exact TI value that is able to suppress the entire longitudinal magnetization in adipose tissue. Further, it is mainly the water proton that is responsible for the opposed-phase effect when employing the combined chemical shift and phase contrast method. Finally, the opposed-phase STIR sequence has some advantages over an in-phase STIR sequence, since it allows for a better signal/noise ratio and more slices.

APPENDIX

The intersection of OPIR and IPIR can be obtained by a numerical analysis using the following formula to express the signal intensity (SI) of an IR sequence, wherein $N(H)$ is the proton density, assuming TE ≪ TR:

$$SI = N(H)\left[1 - 2\exp\left(\frac{-TI}{T1}\right) + \exp\left(\frac{-TR}{T1}\right)\right] \exp\left(\frac{-TE}{T2}\right) \quad (A1)$$

In adipose tissue, the mean water and fat fractions were ~15 and 85%, respectively. The mean density of human fat is 0.9000 g/ml (18), and it contains a negligible amount of fat-free solids. More than 99% of the lipid is triglyceride. Therefore, 1 ml of adipose tissue contains 0.135 g water and 0.765 g triglyceride. The fractions of hydrogen protons in water are ~0.135(2/18) = 0.015. Thus, if the adipose fatty acid is composed solely of oleic acid, the molecular formula will be $C_{60}H_{113}O_6$, and the fraction of the hydrogen proton 0.765(113/929) = 0.093. Therefore,

$$N(H_{fat}):N(H_{water}) \approx 1:0.16$$

The T1 and T2 of the $-CH_2$ and H_2O of adipose tissue were adapted from the study by Luyten et al. (13). These values were obtained from subcutaneous fat by using spatially resolved spectroscopy at 1.5 T:

$T1_{CH_2}$ = 252 ms $T2_{CH_2}$ = 131 ms
$T1_{water}$ = 963 ms $T2_{water}$ = 44 ms

On substituting these numbers in Eq. A1, the SI can be plotted as a function of the TI. In this condition, the intersection of the OPIR and IPIR is then ~175 ms. Various parameters potentially explain the disparity between this figure and the results in normal volunteers. However, the largest contributor to this disparity would be the T1 of the fat.

Acknowledgment: We thank the MR specialists for their technical help.

REFERENCES

1. Byder GM, Young IR. MR imaging: clinical use of the inversion recovery sequence. *J Comput Assist Tomogr* 1985;9:695–75.
2. Dwyer AJ, Frank JA, Sank VJ, Reinig JW, Hickey AM, Doppman JL. Short-TI inversion-recovery pulse sequence: analysis and initial experience in cancer imaging. *Radiology* 1988;168:827–36.
3. Fleckenstein JL, Archer BT, Barker BA, Vaughan JT, Parkey RW, Peshock RM. Fast short-tau inversion-recovery MR imaging. *Radiology* 1991;179:499–504.
4. Dousset M, Weissleder R, Hendrick RE, et al. Short TI inversion-recovery imaging of the liver: pulse-sequence optimization and comparison with spin-echo imaging. *Radiology* 1989;171:327–33.
5. Shuman WP, Lambert DT, Patten RM, Baron RL, Tazioli PK. Improved fat suppression in STIR MR imaging: selecting inversion time through spectral display. *Radiology* 1991;178:885–7.
6. Morse WI, Soeldner JS. The measurement of human adipose tissue mass. In: Renold AE, Cahill GFJ, eds. *Adipose tissue*. Baltimore: Williams & Wilkins, 1965:653–9.
7. Dixon WT. Simple proton spectroscopic imaging. *Radiology* 1984;153:189–94.
8. Bottomley PA, Foster TH, Argersinger RE, Pfeifer LM. A review of normal tissue hydrogen NMR relaxation times and relaxation mechanisms from 1–100 MHz: dependence on tissue type, NMR frequency, temperature, species, excision, and age. *Med Phys* 1984;11:425–48.
9. Jensen KE, Jensen M, Grundtvig P, Thomsen C, Karle H, Henriksen O. Localized in vivo spectroscopy of the bone marrow in patients with leukemia. *Magn Res Imag* 1990;8:779–89.
10. Chen JH, Avram HE, Crooks LE, Arakawa M, Kaufman L, Brito AC. In vivo relaxation times and hydrogen density at 0.063–4.85 T in rats with implanted mammary adenocarcinoma. *Radiology* 1992;184:427–34.
11. Shuman WP, Baron RL, Peters MJ, Tazioli PK. Comparison of STIR and spin-echo MR imaging at 1.5 T in 90 lesions of the chest, liver, and pelvis. *AJR* 1989;152:853–9.
12. Chan TW, Listerud J, Kressel HY. Combined chemical-shift and phase-selective imaging for fat suppression: theory and initial clinical experience. *Radiology* 1991;181:41–7.
13. Luyten PR, Anderson CM, Hollander JA. 1H NMR relaxation measurements of human tissues in situ by spatially resolved spectroscopy. *Magn Res Med* 1987;4:431–40.
14. Szumowski J, Eisen JK, Viniski S, Haake PW, Plewes DB. Hybrid methods of chemical-shift imaging. *Magn Res Med* 1989;9:379–88.
15. Stimac GK, Porter BA, Olson DO, Gerlach R, Genton M. Gadolinium-DTPA-enhanced MR imaging of spinal neoplasms: preliminary investigation and comparison with unenhanced spin-echo and STIR sequences. *AJNR* 1989;9:839–46.
16. Mihara F, Gupta KL. Gd-DTPA-enhanced short repetition time and short inversion time recovery magnetic resonance imaging. *Invest Radiol* 1991;26:734–41.
17. Rosenthal R, Thulborn KR, Rosenthal DI, Kim SH, Rosen BR. Magnetic susceptibility effects of trabecular bone on magnetic resonance imaging of bone marrow. *Invest Radiol* 1990;25:173–8.
18. Fidenza F, Keys A, Anderson JT. Density of body fat in man and other mammals. *J Appl Physiol* 1953;6:252–6.